Polymer Testing 102 (2021) 107340

Contents lists available at ScienceDirect

Polymer Testing

journal homepage: www.elsevier.com/locate/polytest

Bench-scale fire stability testing – Assessment of protective systems on carbon fibre reinforced polymer composites

Weronika Tabaka [a], Sebastian Timme [a], Tobias Lauterbach [a], Lilian Medina [b], Lars A. Berglund [b], Federico Carosio [c], Sophie Duquesne [d], Bernhard Schartel [a,*]

[a] Bundesanstalt für Materialforschung und -prüfung (BAM), Unter den Eichen 87, 12205, Berlin, Germany
[b] Department of Fibre and Polymer Technology, Wallenberg Wood Science Center, KTH Royal Institute of Technology, Teknikringen 56, 100 44, Stockholm, Sweden
[c] Dipartimento di Scienza Applicata e Tecnologia, Politecnico di Torino, Alessandria Campus, Via Teresa Michel 5, 15121, Alessandria, Italy
[d] University of Lille, CNRS, INRAE, Centrale Lille, UMR 8207 – UMET – Unité Matériaux et Transformations, F-59000, Lille, France

ARTICLE INFO

Keywords:
Fire stability
Bench-scale fire resistance testing
Carbon fibre reinforced polymer
Protective coatings

ABSTRACT

Fire resistance testing of components made of carbon fibre reinforced polymers (CFRP) usually demands intermediate-scale or full-scale testing. A bench-scale test is presented as a practicable and efficient method to assess how different fire protective systems improve the structural integrity of CFRPs during fire. The direct flame of a fully developed fire was applied to one side of the CFRP specimen, which was simultaneously loaded with compressive force. Three different approaches (film, non-woven, and coatings) were applied: paper with a thickness in the range of μm consisting of cellulose nanofibre (CNF)/clay nanocomposite, nonwoven mats with thickness in the range of cm and intumescent coatings with a thickness in the range of mm. The uncoated specimen failed after just 17 s. Protection by these systems provides fire stability, as they multiply the time to failure by as much as up to 43 times. The reduced heating rates of the protected specimens demonstrate the reduced heat penetration, indicating the coatings' excellent heat shielding properties. Bench-scale fire stability testing is shown to be suitable tool to identify, compare and assess different approaches to fire protection.

1. Introduction

The increasing interest in carbon fibre reinforced polymers (CFRP) by various industries such as aviation, shipbuilding, the automotive sector, and construction arises from their combination of light weight and outstanding mechanical properties. However, one of the critical issues for using these materials in load-bearing applications is their fire stability. Polymer composites release heat, smoke and toxic fumes when they are exposed to fire, and therefore represent a fire hazard that is typical for polymeric materials. Further, they show a dramatic loss in structural integrity as soon as the glass transition temperature of the polymer matrix, typically located in the range 100–200 °C) is reached, with decomposition occurring between 300 and 400 °C. The polymer matrix softens and decomposes, weakening the composite structure. Furthermore, the simultaneous application of flame and mechanical load leads to immediate distortion and failure of the composite [1–8]. Intact fibres are still able to transfer tensile loads, but not compressive loads, resulting in buckling and the delamination of layers [9–12]. Testing the fire stability of components under realistic conditions typically demands intermediate-scale or full-scale testing. In recent years, few approaches to fire stability testing on the intermediate scale have been reported in the literature [2,3,13,14]. There are also only few studies on fire stability (= mechanical failure under simultaneous fire and mechanical load) in the bench scale [5,15–18]. Over the years, various approaches have been reported to improve the structural integrity of polymer composites in fire [5]. Therefore, we propose to use a bench-scale set-up simulating the key parameters for proper assessment of fire stability, particularly for the practicable assessment of protective concepts during their development. As has been already reported, this method saves time, effort, personnel and costs [18]. The aim of our research was to perform the bench-scale fire stability testing of CFRP composites with three different kinds of protective approaches (film, non-woven, and coatings). The tests were conducted under compression in a fully developed fire (heat flux ≈ 180 kW/m^2).

Fire-retardant coatings are widely used as a fire protection in various areas [19] including building construction [20–23] and transportation [24]. They provide a protective barrier against heat. The superiority of coatings over additives lies in their preservation of the intrinsic

* Corresponding author. Bundesanstalt für Materialforschung und -prüfung (BAM), Unter den Eichen 87, 12205, Berlin, Germany.
E-mail address: bernhard.schartel@bam.de (B. Schartel).

https://doi.org/10.1016/j.polymertesting.2021.107340
Received 19 February 2021; Received in revised form 18 August 2021; Accepted 5 September 2021
Available online 8 September 2021

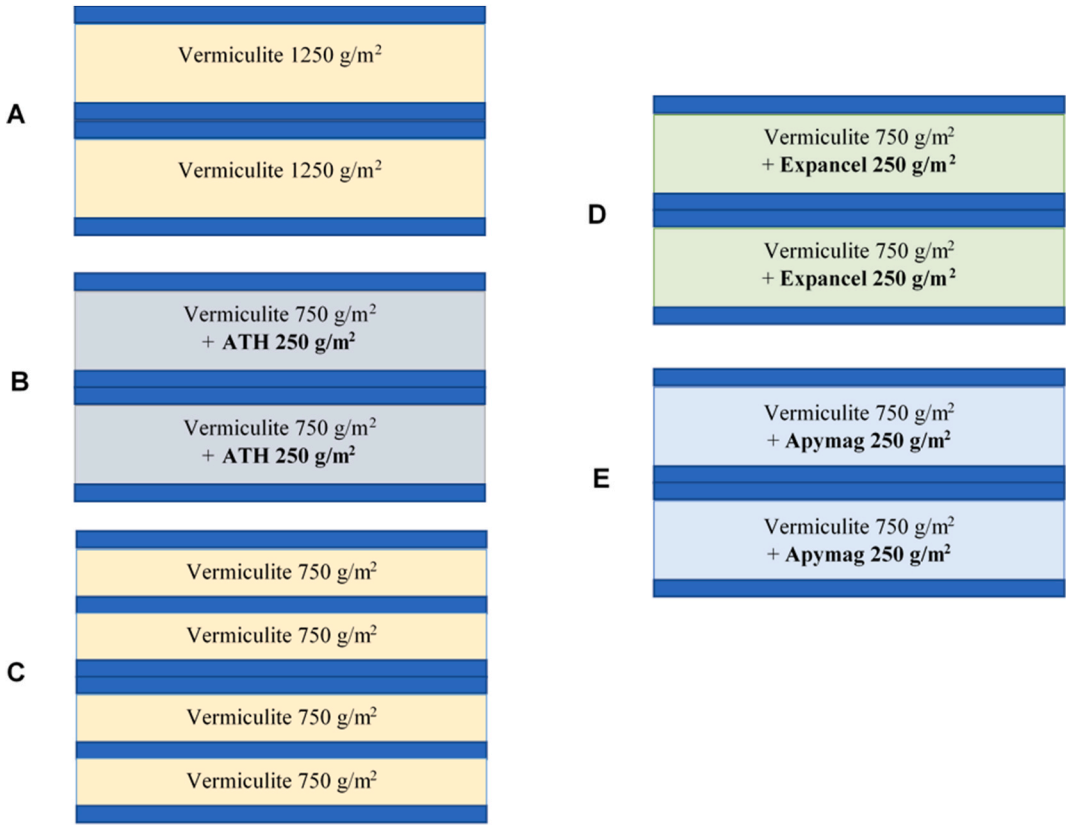

Fig. 1. Schematic set-up of sandwich NW coatings.

properties of the substrate and in the fact that they can be used on multiple substrates [1,25,26]. Three sets of systems selected from different protective approaches were applied to CFRP composites. A recently proposed class of materials chosen as a protective coating are papers consisting of cellulose nanofibre (CNF)/clay nanocomposite which, exhibit a unique brick-and-mortar structure. This set is characterized by remarkable flame-retardant and gas barrier properties [27–33]. The second selected set of protective systems are composed as double sandwiches, with nonwoven fabric (60% basalt, 40% Kermel) as an outer layer and varying inner layers (vermiculite and vermiculite with flame retardants), produced as fire protection for CFRP composite. Kermel is a polyamide-imide fibre shows non-burning and non-melting properties during fire. The FR nonwoven products are mainly used in protective textiles for firefighters and the military. Therefore, they must comply with the most critical requirements [34,35]. The composition of all nonwoven systems is based on vermiculite well known for its 'self--intumescent' properties [36–39]. To improve the fire stability of non wovens, some of the nonwoven systems contain additives. Two systems were prepared by adding two of the most common inorganic hydroxide flame retardants: aluminium trihydroxide (ATH) and magnesium hydroxide (MH). These mineral filler fire retardants decompose endothermically with the release of water in the vapour phase and the formation of protective residue. Furthermore, they are also remarkable smoke suppressors [40–42]. The other additives are Expancel® microspheres that dramatically expand when heated [43,44]. The intumescent coatings typically are composed of four basic ingredients: an acid source, a carbon source acting as a charring agent, a blowing agent and a binder resin. When intumescent coating is exposed to fire, it swells and forms a multicellular char which acts as a protective barrier [45–48]. Intumescent coatings with expandable graphite (EG) were chosen as a third protection approach for CFRP composites. EG produces gas and expands when it is exposed to heat. EG is formed when graphite is intercalated with nitric or sulphuric acid. These coatings are characterized by enormous expansion and are often much more effective than conventional intumescent systems [49–54]. The variety of protective systems featuring different approaches – μm-thick nanostructured clay/CNF papers, bulky nonwoven mats (with thicknesses in the cm range) and thin intumescent coatings (with thicknesses in the mm range) – was chosen to prove the potential of the bench-scale fire testing presented. The protective coatings were not applied as load-bearing layers. They were proposed to slow down the heating up of the CFRP. Extending the time to reach glass transition temperature and decomposition temperature of the resin, respectively, increase the time to mechanical failure in fire.

The fire stability test at the bench scale investigated the performance of CFRP with protective systems, time to failure, and failure mechanism. The goal of this study is to present the bench-scale fire stability test as a practical and feasible method to assess the different protective systems on CFRP composites.

2. Experimental

2.1. Materials

The quasi-isotropic laminate was composed of 24 carbon fibre layers (Tenax – E IMS65 E23 24K Aircraft Quality): [+/−/90/-/0/+/90/0/-/90/+/0]s. Epoxy resin (EPIKOTE™ Resin MGS™ RIMR 935) and curing agent (EPIKURE™, MGS™ RIMH 937) were obtained from Hexion Inc. (Columbus, Ohio, USA). Nanofibrillated cellulose/layered silicates clay (CNF/clay) papers were provided by Politecnico di Turino. The CNF:clay ratio is 50:50. The tests were conducted on three coating specimens with different thicknesses: 90 μm, 95 μm, and 120 μm, respectively. Five (A, B, C, D, and E) multilayer nonwoven systems (NW coatings) composed as double sandwich composites (consisting of two single sandwich composites punched together) were provided by Laboratoire de Génie des Procédés d'Interactions Fluides Réactifs-Matériaux UPRES EA 2698,

Table 1
Intumescent coatings.

Intumescent Coating	Expansion ratio	Thickness/ µm	Fibres	Density/ kg/m^3	Additives
A	10:1	1000	mineral	320	EG
B	20:1	500	mineral + glass	327	EG
C	11:1	665	mineral + glass	350	EG + ATH
D	22:1	665	mineral + glass	966	EG + epoxy resin 30%

Ecole Nationale Supérieure de Chimie de Lille, France. All systems are presented in Fig. 1. The outer layer of the single sandwich was manufactured from nonwoven fabric (60% basalt, 40% Kermel). Basalt fibre, as they are concerned, are mineral fibre presenting better properties compare to glass fibre and being cheaper than carbon fibre. They are widely used in the field of textile fire protection for various applications including aerospace. The inner layers differed for each system. System A has a 'basic' structure and its single sandwich consists of three layers: two outer NW layers and one inner – Vermiculite 1250 g/m^2. Vermiculite ($(MgFe,Al)_3(Al,Si)_4O_{10}(OH)_2{\cdot}4H_2O$) is a hydrous layered silicate material. During heating, bulk vermiculite releases water and immediately expands. System C consists of four 750 g/m^2 Vermiculite layers alternating with six NW layers. Systems B, D and E consist of six layers: four NW layers and one inner – Vermiculite 750 g/m^2 with additives: in system B – aluminium trihydrate 250 g/m^2 (ATH), in system D – Expancel 250 g/m^2, in system E – Apymag 250 g/m^2 (magnesium hydroxide). Expancel® microspheres are small plastic particles with an average diameter of 10–40 µm. When heated, the microspheres expand and increase dramatically in volume – to 40–150 µm. This is caused by gas encapsulated inside the particles, which increases in pressure at higher temperatures (70–200 °C). Furthermore, because microspheres are also highly resilient, they are characterized by enormous resistance to several cycles of loading/unloading without breaking [43,44]. Four commercial intumescent coatings (coating A, coating B, coating C, and coating D) were supplied by Tecnofire®, UK (60852A, 60843A, 60172A, and 67152F) and are characterized in Table 1. They are composed of expandable graphite, high-temperature–resistant mineral fibre and organic binder. Additionally, three of them also contain of some additives (glass fibres, ATH or epoxy resin). Fig. 2 shows digital photos of

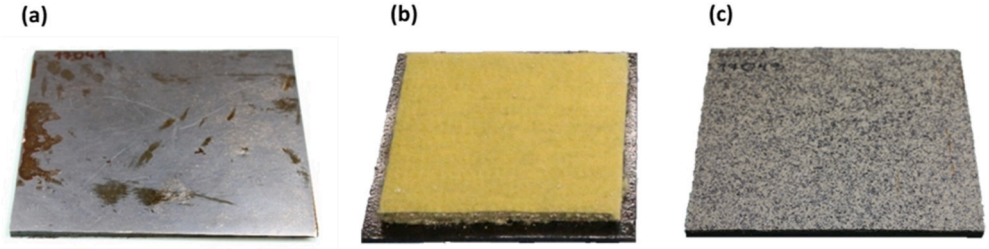

Fig. 2. Representative digital photos of each of the coating systems glued to the CFRP composite: (a) CNF/clay coating, (b) nonwoven system, (c) intumescent coating.

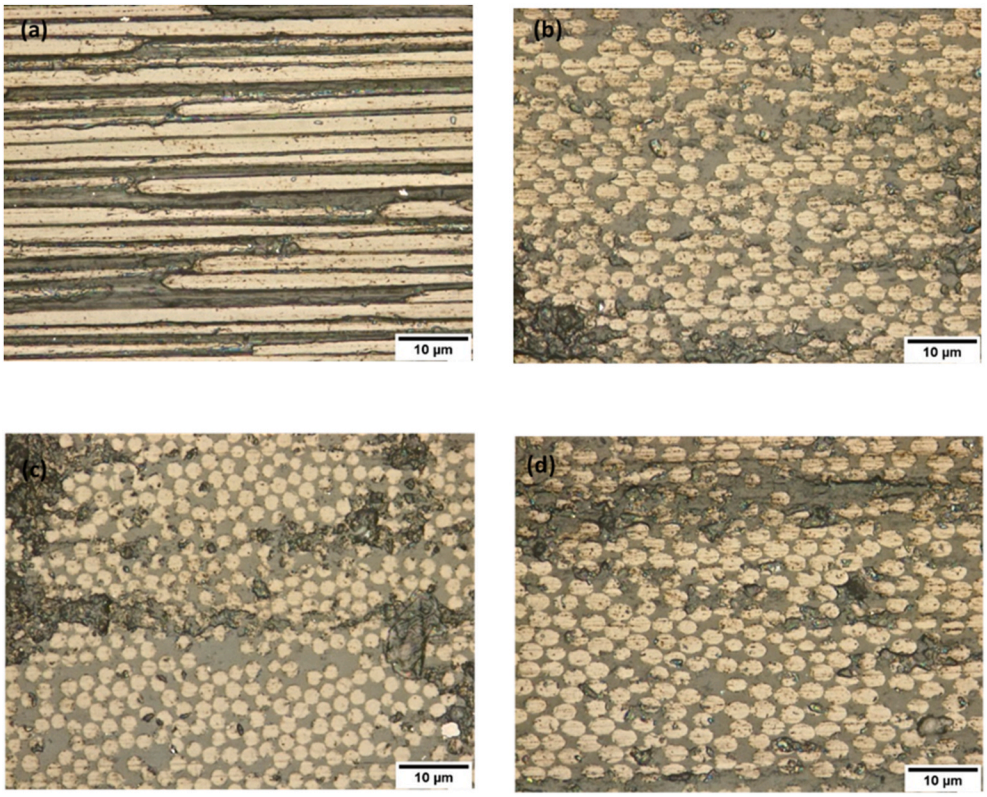

Fig. 3. Optical micrographs of single carbon layers with different orientations: a) 0°, b) 45°, c) 90°, d) 135° taken from the cross-section of laminate.

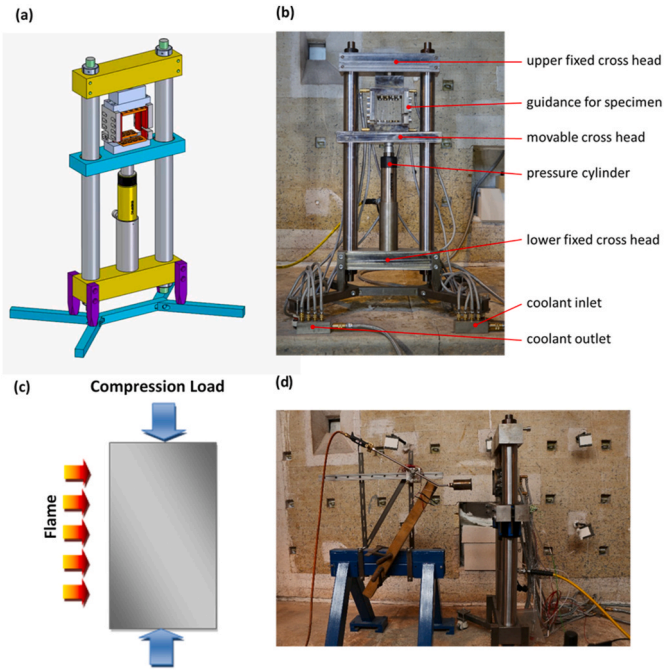

Fig. 4. (a) Isometric view of the bench-scale compression device, (b) bench-scale set-up, (c) scheme of the fire stability test, (d) bench-scale set-up with burner.

each of the protective systems glued to the CFRP composite using the same epoxy resin (EPIKOTE™ Resin MGS™ RIMR 935) during preparation of the composite.

Large (ca. 1200 mm × 600 mm) carbon fibre/epoxy resin composite shells were prepared by Vacuum Assisted Resin Transfer Moulding (VARTM). The moulds were 1470 mm in width and 2900 mm in length and had a curvature diameter of 4150 mm. The curvature corresponds to the typical shell structure used for the fuselage in aviation. The quasi-isotropic laminate consists of 24 carbon-fibre layers which are oriented in four different angles (0°, 45°, 90°, 135°) and has thickness of 3 mm. The composite was cut by drilling machine (LaserComb GmbH, Germany) into 120 mm × 120 mm (laminates with intumescent and CNF/clay coatings) and 145 mm × 150 mm (laminates with nonwoven systems) specimens. The thin film of epoxy resin was applied to the specimens and the coatings were placed upon them. To cure the resin, which provided the permanent joining, the composites were kept at 160 °C for 5 h (laminates with intumescent and CNF/clay coatings) and at 120 °C for 8 h (laminates with nonwoven systems). Fig. 3 presents the optical micrographs of single carbon layers with different orientations, which were taken from the cross-section of the laminate.

2.2. Scanning Electron Microscopy

The gold-coated cross-sections of the CF/epoxy resin laminates as well as the fire residues were investigated by Scanning Electron Microscopy.[55] The micrographs were taken using a Zeiss EVO MA 10 (Zeiss, Germany). The Electron High Tension (EHT) voltage used in measurement was 15 V.

2.3. Bench-scale fire stability test: conception, construction, principle

The most critical issue for carbon fibre reinforced polymer composites in load-bearing applications is their fire stability. As soon as the glass transition temperature of the polymer matrix is reached, the mechanical properties of composites deteriorate. Polymeric composites lose their structural integrity and can easily fail under external compression load. The principal fire stability test was based on the simultaneous application of mechanical load and fully developed fire directly to the one side of CFRP composite. Carbon fibres still transfer tensile loads quite well also after the glass transition temperature of the matrix has been reached. Therefore, compressive loading was chosen as the mechanical loading for the test, because components under compression and fire are less tolerant of failure. Compression failure appears as micro-buckling or delamination and cracking of the specimen [2].

The compression device was designed to resist up to more than 230 kN (Fig. 4). The specimen is clamped at the top and the bottom and guided along the side edges. The functional principle is deduced from the 'compression after impact' (CAI) fixture (ASTM D 7137). The original CAI construction was crucially improved through mirroring above the specimen. To allow deformation during the tests, a section along the sides was left unsupported. To hinder buckling, these gaps were left in the lower third of the guides. Further, using different guides to support the front and the back of the specimen ensured that the unsupported range on the back was supported on the front and vice versa. The compression device was originally constructed of welded components and connected by screws to accommodate up to 150 mm × 150 mm specimens. The additional set-up allows 120 mm × 120 mm specimens to be examined as well. The compression loads are adjusted by Enerpac RC-106 pressure cylinders, which exert a maximal compressive force of 101.5 kN. The pressure cylinders are easily exchangeable. The larger Enerpac RC-256 cylinder is able to exert the maximal compressive force up to 230 kN. The clamps and guides exposed to fire were equipped with an integrated water-cooling system to prevent unintended thermal expansion. Fig. 4a and b presents the bench-scale set up.

Load is applied by a hydraulic machine in the form of compression and fire by a propane gas burner (nozzle diameter 60 mm) directly to one side of the specimen (Fig. 4c and d). The burner was connected to an EL-FLOW® Metal Sealed Gas Mass Flow Meter (Bronkhorst High-Tech B. V., Netherland), which provided a constant flow of gas. During the experiment, the integrated water-cooling system was switched on in the vicinity of direct fire exposure. First, a static load test was conducted at room temperature without any fire and the ultimate failure load of the CF/epoxy resin laminate was determined. The compression load selected for the bench-scale fire stability testing was 10% of the ultimate failure load. Such a relative low percentage of the ultimate failure load increases time to mechanical failure during fire as well as amplifying the differences between different materials [2,3,18]. Thus, the chosen testing parameter aims at investigating the thermo-structural response of the composites and to achieve reliable results. Nevertheless, it still corresponds to realistic demands for the fire stability that are different for the different applications and may usually between 10% and 70%. The flame application chosen in the bench scale corresponds well to the flame application of fire tests used in aviation, e. g. 14 CFR 25.856 Appendix F Part VII; 2003 using a NextGen burner. The flame application was adjusted before the test and the proper heat flux (180 kW/m^2) and the temperature (about 1020 °C) were adjusted by varying the gas flow. The distance between the burner and the sample was kept constant at 27.5 cm. The heat flux meter, a water-cooled Vatell Thermogage® TG1000-1 (Gardon gauge type, Serial #9829, calibration accuracy 3%), was placed in a hole drilled in the middle of a ceramic reference plate (Fiberfrax® Duraboard®, thickness 10 mm). The thermocouple gauge was located next to the heat flux meter.

During a fire test, the temperature was measured by thermocouples type K located on the back surface of the specimen. One thermocouple was glued in the centre of laminate sample with high-temperature resistance ceramic adhesive. Before the fire experiment, the burner was warmed up for 30 s and then swivelled to the specimen. A special trigger was installed at the burner, which indicated when the flame was applied to the specimen. When the specimen buckled, the burner was returned to the initial position and the test was finished.

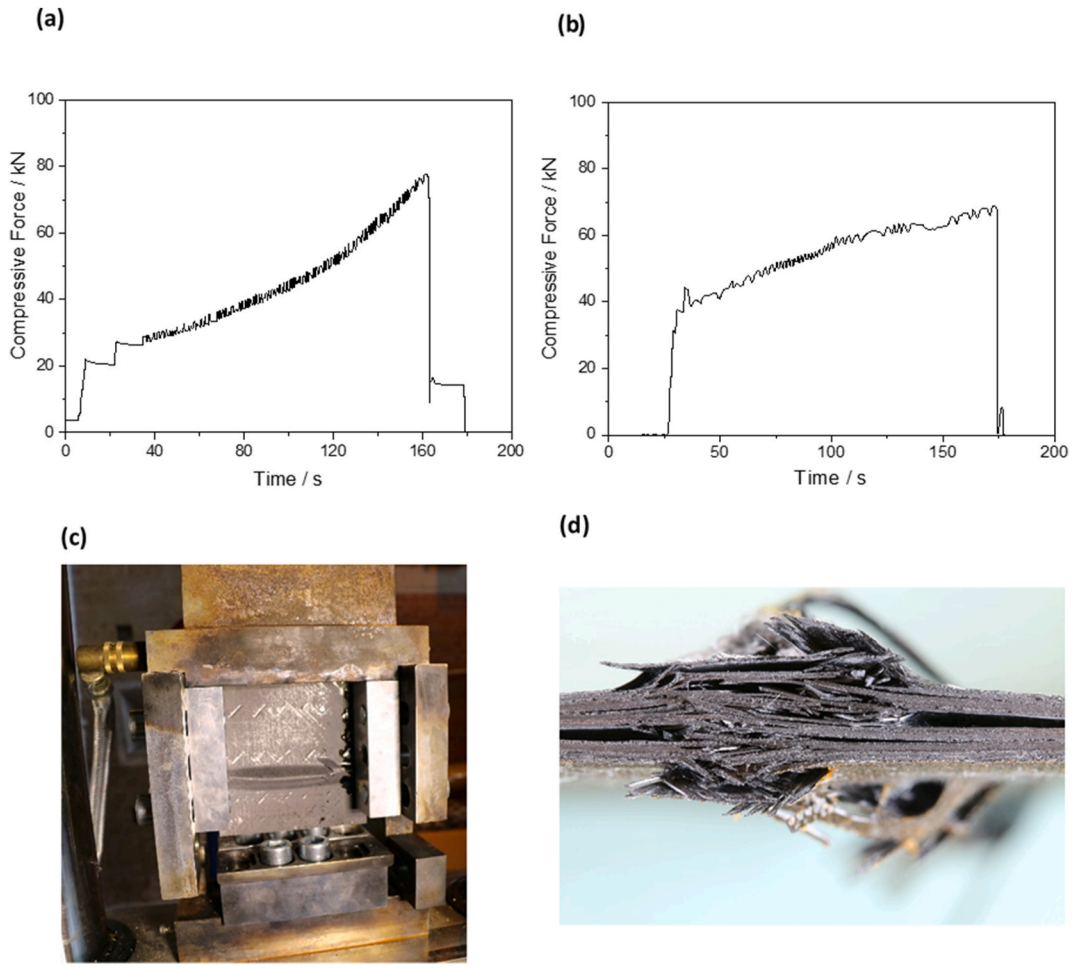

Fig. 5. Compressive force of CF/epoxy resin as a function of time for two laminates (a) with the size later used for CNF/clay and intumescent coatings, (b) with the size later used for nonwoven protective mat sandwiches; (c) CF/epoxy resin laminate after failure load test in bench-scale set-up at room temperature mounted to the compression device, (d) lateral view.

3. Results and discussion

3.1. Static load test

The mechanical properties of carbon fibre reinforced epoxy resin laminate shells (CFRP) were investigated in a bench-scale test at room temperature. The compressive force was increased until the ultimate failure load was reached. Initially the composite showed linear elastic behaviour. The fracture process was initiated when the maximum resistance of laminate was exceeded. The main failure mechanism of laminate shells under compressive loading was observed to be buckling. Fig. 5a and b presents the results for the specimens without protection. The failure of the specimens occurred at 81.0 ± 4.5 kN (CFRP laminates used for composites with CNF/clay and intumescent coatings) and 68.8 kN (laminates used for composite with nonwovens). The deviation in the ultimate failure load is a result of the different specimen sizes and thickness. The main parameter that influences the buckling load, according to the buckling analysis by Hertel, is width, here 120 mm and

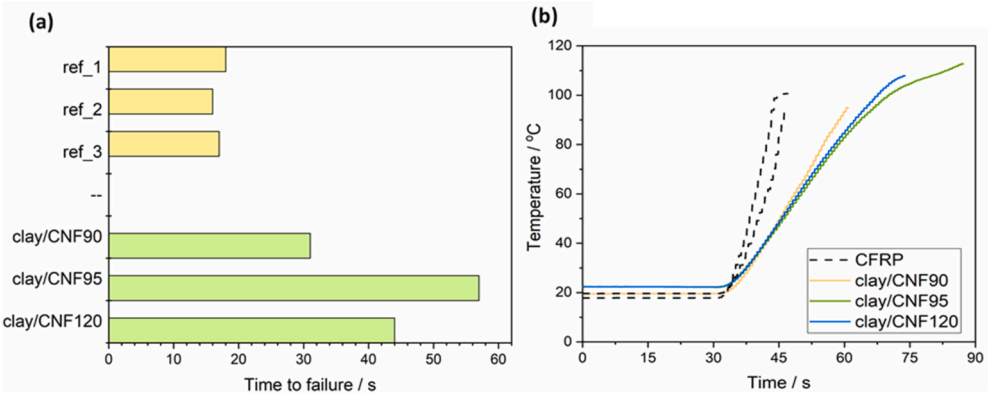

Fig. 6. (a) Comparison of time to failure and (b) temperature profiles of CFRP laminates without and with CNF/clay coatings.

Table 2
Results for laminates with CNF/clay coatings at the moment of failure.

	Time to failure/s	Temperature on back at failure/°C	Slope – heating rate /°C/s
CFRP	17 ± 1	98 ± 16	4.2 ± 0.1; 5.7 ± 0.1
+ CNF/clay90	31	95	2.9 ± 0.1
+ CNF/clay95	57	113	2.3 ± 0.1
+ CNF/clay120	44	108	2.3 ± 0.1
+ CNF/clay (averaged)	44 ± 13	105 ± 10	2.5 ± 0.4

150 mm, respectively. The critical buckling load decreases as width increases [3]. Fig. 5c and d presents the photos of the buckled specimen after a failure load test. Fig. 5c shows the laminate shell mounted to the compression device. Fig. 5d displays a lateral view of the sample. The arrangement of the carbon fibres after failure is visible, indicating that delamination buckling was a failure process for this composite. This interlaminar failure is characterized by propagation of cracks parallel to the loading direction. The amount of delamination and buckling of layers increased until each layer was crushed – subjected to transverse fracture [56].

3.2. Bench-scale test: fire performance – CFRP laminate with CNF/clay coatings

Fire tests were performed with the bench-scale test set-up in the compression device, applying 10% of failure load at room temperature (~8.1 kN). The load was kept constant and applied prior to and during application of flame until the specimen failed. Failure was observed when the applied load was no longer supported by the specimen, which occurred when sample buckled. The time between application of flame and the total loss of mechanical stability was defined as the time to failure. The testing conditions for each specimen were identical (settings to control the burner and servo-hydraulic testing machine). Therefore, the main influence on the different performances of the samples is the thickness of the coatings applied. A comparison of time to failure for reference CFRP specimens and those protected by CNF/clay coating is presented at Fig. 6a.

The recorded data on failure are given in Table 2. Three specimens of CFRP laminate without coating failed at between 16 s and 18 s. This low

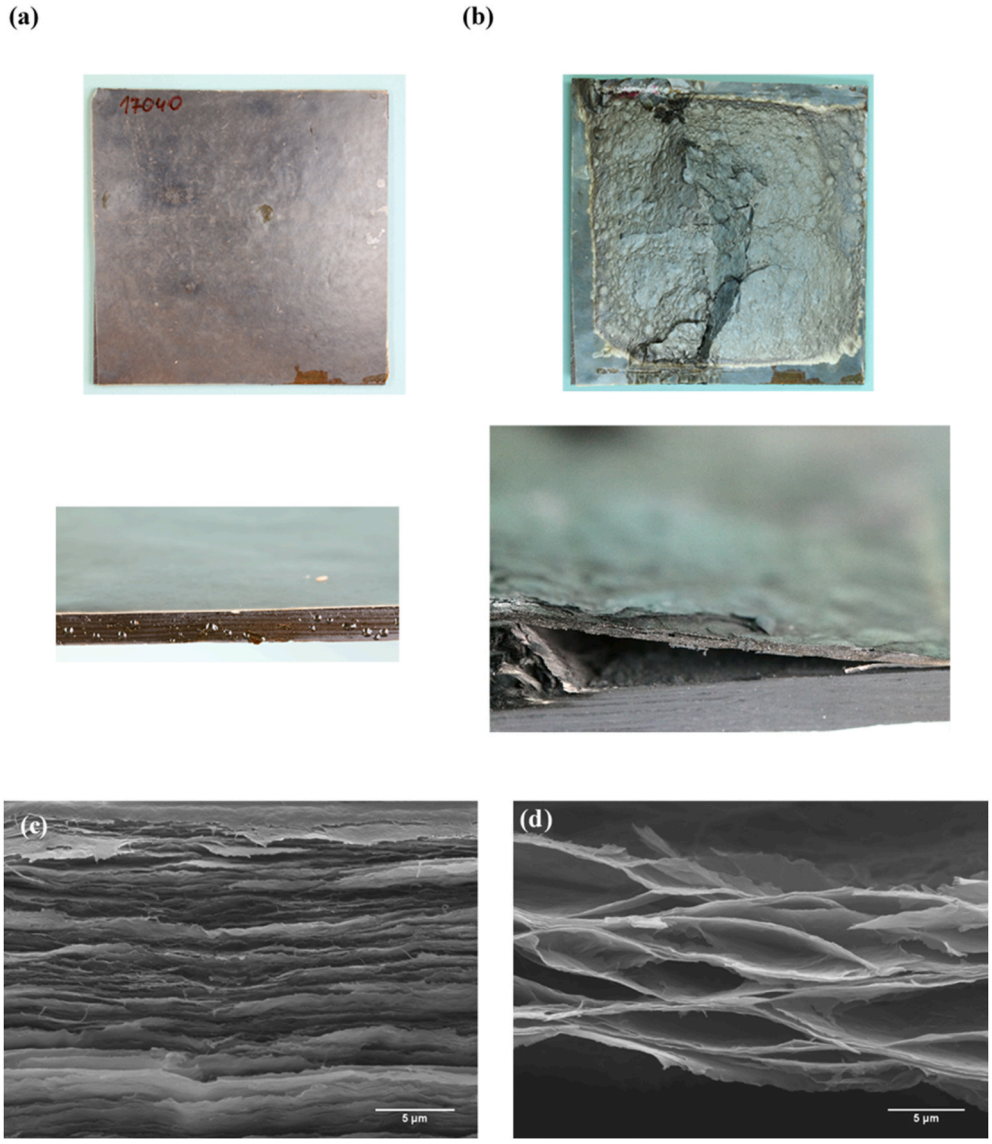

Fig. 7. Digital photos, top view and side view of CFRP with CNF/clay paper (a) before and (b) after burning in the bench-scale test. SEM images of cross-sections of CNF/clay paper before (c) and after (d) bench-scale test.

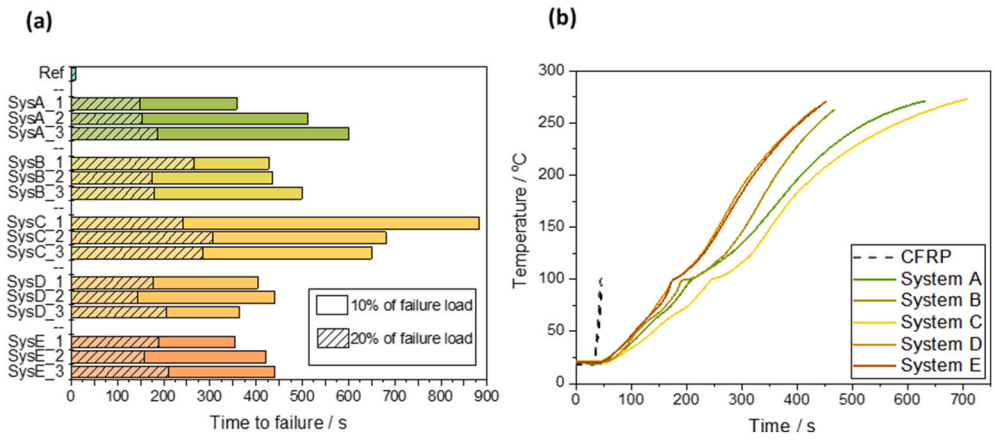

Fig. 8. (a) Comparison of time to failure of each of the systems for laminates with nonwoven protective systems; (b) temperature profiles on the back of each system without and with nonwoven protective system.

uncertainty indicates the high-quality fabrication of the specimens, as well as the high repeatability of testing at the bench scale. Since the coatings insulated the CFRP laminates, the thermal softening and decomposition rates of the substrate were slowed. Consequently, the specimens with coatings maintained their structural integrity longer and the time to failure was prolonged. The protection effect is attributed mainly to the oriented clay nanoplatelets. The specific alignment of clay (or MMT, montmorillonite) in nanocellulose paper allows the heat transfer rate to be reduced through the formation of a heat shield. It also promotes the char production of CNF. The 'brick and mortar' CNF/clay structure functions as a barrier and reduces pyrolysis products/fuel [32,33]. This system, around 100 μm-thick, achieved an average improvement in time to failure of 258% over uncoated CFRP specimens (~44 s). The longest time to failure 57 s was achieved by the sample with a coating 95 μm –thick. The temperature on the back at the moment of failure was higher for specimens with coatings than for pure CFRP composite. This result is consistent with the effect of reduced heat penetration combined with the prolonged time to failure. The drop in temperature inside the specimen with increasing distance from the surface becomes more moderate, as the specimen is heated more homogenously with a lower heating rate over a longer time. The temperature was measured by a thermocouple attached to the back of specimens. The pure CFRP plates reached ~97.5 °C at the moment of failure. Fig. 6b shows the temperature rise on the back of the specimens measured by thermocouples during fire exposure of pure CFRP laminate and with CNF/clay coatings. The curves show the temperature profiles up to failure. The coatings provided effective insulation for CFRP laminates, which is visible in their significant influence on the heating rates. The most important parameter that influences the performance of the coating as an insulative barrier is heat conductivity. The thermal expansion of the material in the through-thickness direction is non-uniform due to a thermal gradient. It is highest at the hot surface and decreases with the distance from the flame source. The rate of steady conduction heat transfer for a flat plate is described by Fourier's law of conduction:

$$(\dot{Q}_{cond})_{plane} = k_t A\left(\frac{T_{hot} - T_{back}}{\Delta x}\right)$$

where $(\dot{Q}_{cond})$ is the conduction heat transfer rate, k_t is the thermal conductivity of the material, A is the cross-sectional area perpendicular to the heat transfer direction, and Δx is the thickness of the specimen. Therefore, the conduction heat transfer rate depends on the thickness and type of the coating as well. The specimens with coatings are characterized by temperature-time curves with lower slopes, which is attributed to the reduction in heat absorption by the protected CFRP [57,58]. The values of the slopes are shown in Table 2. The slope for CF/epoxy/clay CNF95 is presented in two stages. The heating rate over 100 °C is clearly reduced, most probably due to the volatile pyrolysis gases released within the CFRP shell and to delamination, which cools down the specimen and decreases thermal conductivity [1,10]. Fig. 7a and b presents the digital photos of CFRP laminate with CNF/clay paper 95 μm thick before and after fire stability tests at the bench scale. The observed increase in thickness indicates the expansion of the coating, which protected CFRP laminate from fire and therefore prolonged time to failure. The lateral view of a burnt specimen reveals the dense, layered structure of the coating. As mentioned before, this is also confirmed by the appearance of a 'brick and mortar' structure which provides the thermal barrier protection. The structure of the residue was also stiff and brittle. The highly ordered structure of cellulose influenced the formation of the char, which was thermally stable. Fig. 7c and d displays SEM images of a cross-section of CNF/clay coating before and after burning. The SEM micrograph of the residue shows microscale voids in the structure. During degradation CNF released volatile products, which were hindered by the clay barrier, resulting in the formation of voids at microscale. This caused the structure to expand in the direction of thickness, the delamination of nanopaper, and a further reduction in thermal conductivity. Therefore, CNF/clay coating provides insulation to volatiles and greatly reduces heat transfer [29–33].

3.3. *Bench-scale test: fire performance – CFRP laminate with nonwoven systems*

Fig. 8a presents the time to failure of CFRP reference specimens and specimens with nonwoven protective systems at load levels of 10% and 20%. The higher compressive load (20%) resulted in time to failure only half as long as those than at 10%. Furthermore, there is no major difference in time to failure between specimens testing at the 20% load level. The increasing time to failure with application of decreasing load levels was already reported by Hörold [2]. All systems show outstanding improvement in the fire stability of composites. Protection by coatings played an especially important role in isolating the specimen from the high heat flux. Therefore, they yielded times to failure enhanced by as much as 43 times. The longest time to failure at 10% was achieved by system C with four vermiculite layers (in which each layer has an area density of 750 g/m^2) = ca. 740 s. The area density, which also indicates the thickness of the nonwoven systems, had an influence on the fire stability. Increasing thickness provides a better barrier to hinder heat penetration.

NW coating A contains two vermiculite layers, but the area density of each layer was greater (1250 g/m^2), making the total area density of nonwoven just slightly lower at 0.8. This resulted in a time to failure 0.7 times shorter for than system C. The time to failure of systems with the

Table 3
Results for laminates with nonwoven protective systems at the moment of failure. Compression loads of 10% and 20% of the ultimate failure load were used.

	Time to failure at 10%; at 20%/s	Slope - heating rate/°C/s
CFRP	17 ± 1; 10 ± 1	5.0 ± 0.7
+ **NW System A**	490 ± 122; 163 ± 21	0.5 ± 0.1
+ **NW System B**	454 ± 39; 207 ± 52	0.6 ± 0. 1
+ **NW System C**	737 ± 128; 278 ± 34	0.4 ± 0.1
+ **NW System D**	403 ± 39; 176 ± 31	0.7 ± 0.1
+ **NW System E**	405 ± 46; 186 ± 27	0.7 ± 0.1

additives ATH (System B), MH (System E) and Expancel Microspheres (System D) was more or less equivalent, with an average improvement of ~2500% over uncoated CFRP specimens. Although these nonwoven systems contain only two vermiculite layers with a lower area density (750 g/m^2), the time to failure of load-bearing composites was only 1.2 times shorter than for system A. Flame retardants (in system B, D and E) affect the heat conductivity of the NW coating, which allows similar times to failure to be achieved with lower area density. The average values of time to failure at load levels of 10% and 20% are presented in Table 3.

Fig. 8b presents the temperature profiles of uncoated and coated CFRP specimens with nonwoven protective systems. The systems protected specimens from fire, explaining the slower heating rates. The slopes of the curves which are attributed to the heating rates are shown in Table 3. The NW coatings reduce the heating rates by as much as ~8.5 times. The time before the temperature starts to increase is shifted by approximately 20 s, indicating that the protective system significantly delayed the transition of heat flow through the CFRP plate. The specific 'bending point' around 100 °C is noticeable for CFRP specimens with nonwoven protective systems. At this temperature the volatile gases within the CFRP shell are released, coupled with the softening of the epoxy resin matrix, causing the delamination of the individual CFRP layers. Therefore, the trapped volatile gases considerably reduced thermal conductivity in the direction of thickness [1,10,59]. The temperature profiles also show the temperature at which failure occurred. It was about 2.5 times higher for the specimens protected with nonwoven protective systems. NW coating behaved as a thermal insulation and the specimen had more time to warm up more moderately and more homogenously over its thickness, reaching a much higher temperature at the rear side when it failed. Fig. 9 displays digital photos of CFRP laminates with nonwoven mat systems before and after the fire test. After cooling down, the system still exhibited a flexible, dense, closed structure without holes, which provides a better protection effect.

Table 4
The results for laminates with intumescent coatings at the moment of failure.

	Time to failure at 10%/s	Temperature at failure/°C
CFRP	17 ± 1	89 ± 16
+ **coating A**	176 ± 23	155 ± 5
+ **coating B**	125 ± 24	142 ± 9
+ **coating C**	80 ± 19	114 ± 19
+ **coating D**	116 ± 6	107 ± 3

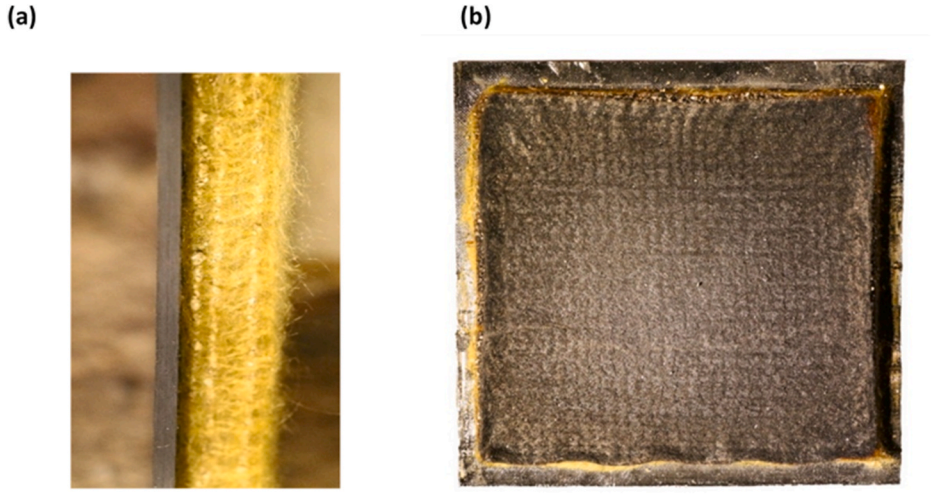

Fig. 9. Digital photos of CF/epoxy resin laminates with a nonwoven (a) before and (b) after the burning test.

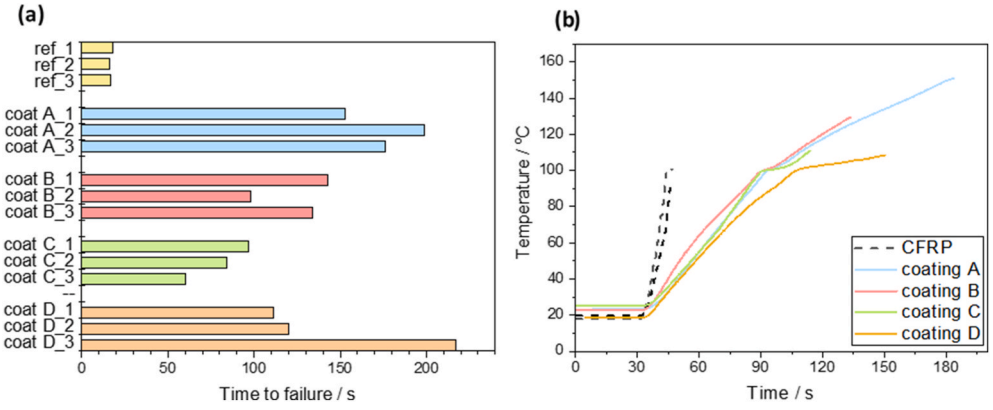

Fig. 10. (a) Comparison of time to failure of CFRP laminates with intumescent coatings; (b) temperature profile of each of the systems.

Table 5
The values of slope – heating rates from temperature profiles.

	Stage 1	Stage 2	Stage 3
CFRP 1	4.2 ± 0.1		
CFRP 2	5.7 ± 0.1		
Coating A	1.4 ± 0. 1	0.55 ± 0.10	0.55 ± 0.10
Coating B	1.4 ± 0. 1	0.4 ± 0.1	0.7 ± 0.1
Coating C	1.4 ± 0. 1	0.25 ± 0.10	0.9 ± 0.1
Coating D	1.1 ± 0.1	0.2 ± 0.1	0.2 ± 0.1

3.4. Bench-scale test: fire performance – CFRP laminate with intumescent coatings

Fig. 10a shows a comparison of the time to failure of pure CFRP plates to specimens with intumescent coatings. The results on the moment of failure (time and temperature at failure) are presented in Table 4. The coatings showed pronounced intumescence and significantly prolonged fire stability. The longest time to failure was observed for the specimen with the greatest thickness (coating A) = ca. 175 s. This coating provided a remarkable improvement of up to 1000% in time to failure. The thickness of the other coatings was only half; hence their time to failure was shorter. Coatings B and D have an expansion ratio twice as high as coating A. However, as was observed, expansion ratio is not as important a factor as the coating thickness. All three of the specimens with glass fibres achieved similar times to failure. Moreover, a slightly shorter time to failure was obtained by the specimen with coating C, which contained ATH. The addition of 30% epoxy resin did not show any significant effect on fire stability. However, coating D was characterized by considerably higher rigidity than the other coatings. The formation of an intumescent layer by coatings effects low thermal

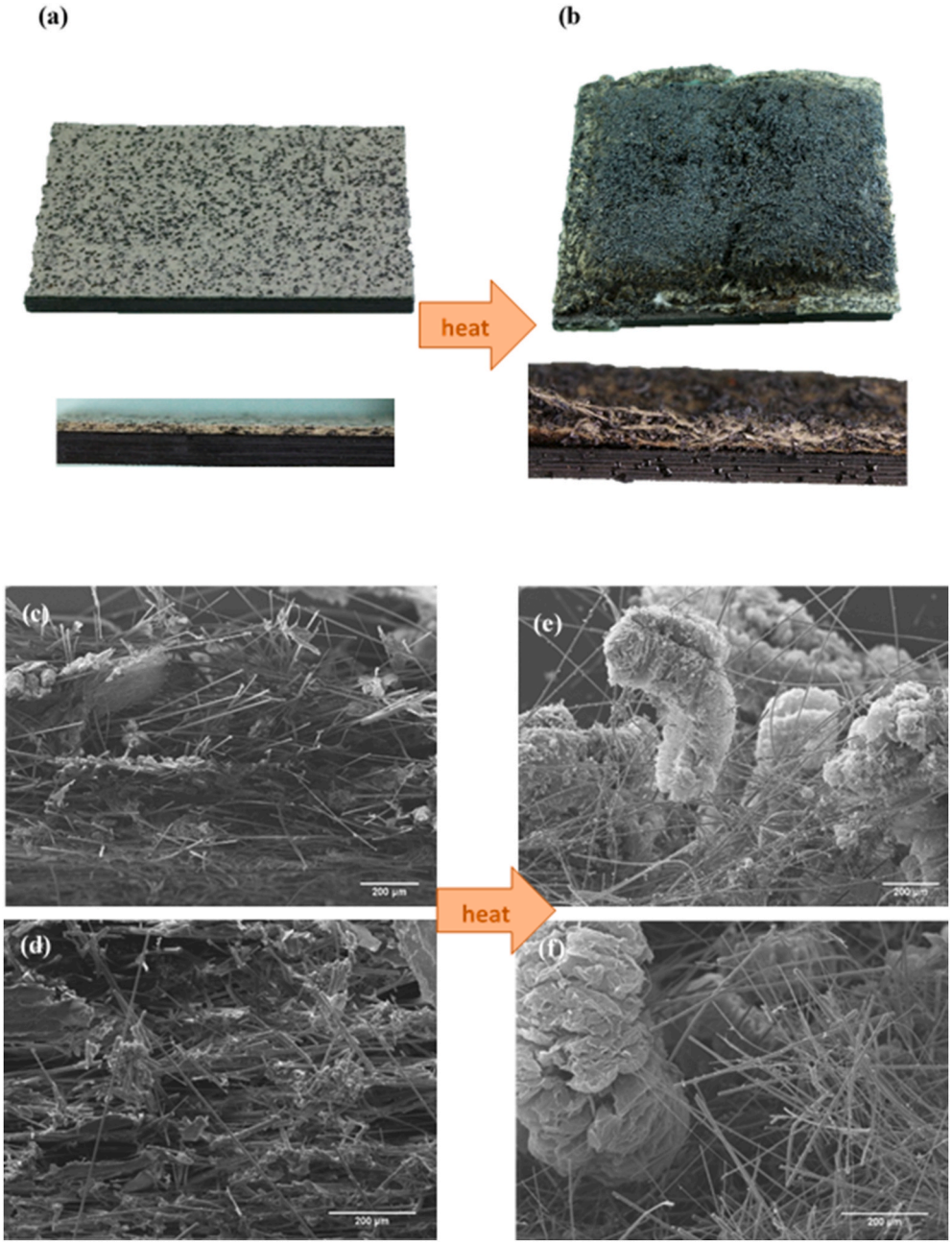

Fig. 11. Digital photos of CF/epoxy resin laminate shells with intumescent coating A (a) before and (b) after burning in the bench-scale test. SEM images of cross-sections of intumescent coating before (c–d) and after (e–f) bench-scale test.

conductivity and furthermore extends the time of maintaining the mechanical support in fire.

Fig. 10b shows the temperature profile of uncoated and coated CFRP specimens with intumescent coatings. The coatings are characterized by excellent protective properties, which is noticeable in the lower heating rates. The specific 'bending' point around 100 °C, which appears in curves for coated specimens, is related to the cooling effect from the outflow of volatile gases, generated by decomposition of the polymer matrix [1,10,59]. The values for the slope, which constitutes the heating rates, are shown in Table 5. Temperature profiles of specimens with coatings were analysed in 3 stages: before, during and after decomposition of the polymer matrix (which occurred when 100 °C was measured on the back of the specimen). Dramatic reductions in heating rates were observed from stage 1, which were 3.7 times lower than reference CFRP specimens. The cooling effect from volatile gases had an additional influence on the reduction of the heating rates in the next stages. Fig. 11a and b shows digital photos of CFRP laminate with coating A before and after burning. A significant increase in the thickness of the coating is observed. Also visible on top of the coating is char, which provided additional insulation to the underlying material. This indicates that EG worked not only as a blowing agent, but also as a charring agent. In the picture of the cross-section of the burnt specimen, swollen EG is clearly visible between mineral fibres. Fig. 11c and d presents SEM micrographs of cross-sections of intumescent coating before and after burning. Pictures before burning show mainly mineral fibres. SEM images after burning exhibit enlarged EG particles adjacent to fibres. The EG during heating formed the worm-like and exfoliated structure, which inhibited heat penetration and may somehow have suppressed mass transfer. This successfully delayed the degradation of matrix and prolonged the time to failure [50,52,60].

4. Conclusions

The main goal of this study was to present a bench-scale test as a suitable tool to investigate the improvement of the structural integrity of CFRP composites with fire protective systems (film, nonwoven mats, and coatings) in a fully developed fire. Therefore, three different approaches were selected. Protective systems play a significant role in the thermal insulation of materials. However, before any application their efficacy must be confirmed by fire testing, which is usually time consuming and expensive. Although bench-scale tests are limited with respect to assessing the performance of components and structures, they are valuable in the assessment of different materials' concepts. Therefore, three different fire protective systems were applied to CFRP composite plates. Their structural integrity in fire was tested at the bench scale. The diversity of investigated approaches emphasised the multiple capabilities of small-scale testing. Results presented the incredible enhancement and prolongation of time to failure of specimens with protective systems, and furthermore, improvement in fire stability. As presented above, even very thin CNF/clay nanostructured paper forms an excellent heat shield and allows CFRP composite to maintain structural integrity much longer in case of fire. It has been observed that the thickness of coatings is a very important parameter that influenced the magnitude of the prolongation of time to failure. However, the structure and this same heat conductivity of the materials used also play an important role. The protective coatings formed a barrier and prevented direct contact between the flame and the specimen surface. This slowed down pyrolysis and the softening of the matrix. The reduced heating rates indicate that protective systems hindered heat penetration through the CFRP plate and provided tremendous insulation. The bench-scale test also allows the investigation of different mechanisms of protection by coatings. The reduced effort of conducting bench-scale tests (lower costs, time, and personnel resources) makes it more practical and effective than intermediate- or large-scale testing. The simple method proposed in this paper can be also used to improve the design of fire protective systems or composites in later research.

Data availability

Data is available upon request.

CRediT authorship contribution statement

Weronika Tabaka: Conceptualization, Investigation/measurements, Analysis/scientific discussion, Writing – review & editing. **Sebastian Timme:** Investigation/measurements, Conceptualization, testing, Analysis/scientific discussion. **Tobias Lauterbach:** Material/specimen preparation, Investigation/measurements. **Lilian Medina:** Advanced material/specimen preparation. **Lars A. Berglund:** Conceptualization nanopapers. **Federico Carosio:** Conceptualization nanopapers, Advanced materials support. **Sophie Duquesne:** Conceptualization nonwoven mats, Advanced materials support. **Bernhard Schartel:** Conceptualization, Writing – review & editing, Analysis/Scientific discussion, Supervision.

Declaration of competing interest

The authors declare that they have no known competing financial interests or personal relationships that could have appeared to influence the work reported in this paper.

Acknowledgements

The authors are grateful to P. Klack for his help.

References

[1] A.P. Mouritz Ap, A.G. Gibson, Fire Properties of Polymer Composite Materials, Springer, Dordrecht, Netherlands, 2006.
[2] A. Hörold, B. Schartel, V. Trappe, M. Korzen, M. Naumann, Structural integrity of sandwich structures in fire: an intermediate-scale approach, Compos. Interfac. 20 (2013) 741–759.
[3] A. Hörold, B. Schartel, V. Trappe, V. Gettwert V, M. Korzen, Protecting the structural integrity of composites in fire: intumescent coatings in the intermediate scale, J. Reinforc. Plast. Compos. 34 (2015) 2029–2044.
[4] A.P. Mouritz, S. Feih, Z. Mathys, A.G. Gibson, Mechanical property degradation of naval composite materials, Fire Technol. 47 (2011) 913–939.
[5] A.G. Gibson, P.N.H. Wright, Y.S. Wu, A.P. Mouritz, Z. Mathys, C.P. Gardiner, The integrity of polymer composites during and after fire, J. Compos. Mater. 38 (2004) 1283–1307.
[6] R.J. Asaro, B. Lattimer, W. Ramroth, Structural response of FRP composites during fire, Compos. Struct. 87 (2009) 382–393.
[7] J.V. Bausano, J.J. Lesko, S.W. Case, Composite life under sustained compression and one sided simulated fire exposure: characterization and prediction, Compos. Part A-Appl. Sci. Manufact. 37 (2006) 1092–1100.
[8] S. Braiek, A. Ben Khalifa, R. Zitoune, M. Zidi, M. Salem, Fire behaviour of hybrid filament-wound single and adhesively bonded composites tubes under static pressure, Polym. Test. 91 (2020), 106815, https://doi.org/10.1016/j.poiymertesting.2020.106815.
[9] L.A. Burns, S. Feih, A.P. Mouritz, Compression failure of carbon fiber-epoxy laminates in fire, J. Aircraft 47 (2010) 528–533.
[10] S. Feih, Z. Mathys, A.G. Gibson, A.P. Mouritz, Modelling the tension and compression strengths of polymer laminates in fire, Compos. Sci. Technol. 67 (2007) 551–564.
[11] A. Anjang, V.S. Chevali, E. Kandare, A.P. Mouritz, S. Feih, Tension modelling and testing of sandwich composites in fire, Compos. Struct. 113 (2014) 437–445.
[12] S. Feih, A.P. Mouritz, Z. Mathys, A.G. Gibson, Tensile strength modeling of glass fiber-polymer composites in fire, J. Compos. Mater. 41 (2007) 2387–2410.
[13] S. Timme, V. Trappe, M. Korzen, B. Schartel, Fire stability of carbon fiber reinforced polymer shells on the intermediate-scale, Compos. Struct. 178 (2017) 320–329.
[14] A. Hörold, B. Schartel, V. Trappe, M. Korzen, J. Bünker, Fire stability of glass-fibre sandwich panels: the influence of core materials and flame retardants, Compos. Struct. 160 (2017) 1310–1318.
[15] A.G. Gibson, T.N.A. Browne, S. Feih, A.P. Mouritz, Modeling composite high temperature behavior and fire response under load, J. Compos. Mater. 46 (2012) 2005–2022.
[16] A.G. Gibson, S. Feih, A.P. Mouritz, Developments in characterising the structural behaviour of composites in fire, in: M. Nicolais, M. Meo, E. Milella (Eds.), Composite Materials, Springer, London, 2011, pp. 187–218.
[17] A.G. Gibson, M.E.O. Torres, T.N.A. Browne, S. Feih, A.P. Mouritz, High temperature and fire behaviour of continuous glass fibre/polypropylene laminates, Compos. Part A-Appl. Sci. Manufact. 41 (2010) 1219–1231.

[18] B. Schartel, J.K. Humphrey, A.G. Gibson, A. Hörold, V. Trappe, V. Gettwert, Assessing the structural integrity of carbon-fibre sandwich panels in fire: bench scale approach, Compos. B Eng. 164 (2019) 82–89.
[19] E.D. Weil, Fire-protective and flame-retardant coatings—a state-of-the-art review, J. Fire Sci. 29 (2011) 259–296.
[20] H. Vandersall, Intumescent coating systems, their development and chemistry, J. Fire Flammability 2 (1971) 97–140.
[21] M. Bartholmai, B. Schartel, Assessing the performance of intumescent coatings using bench-scaled cone calorimeter and finite difference simulations, Fire Mater. 31 (2007) 187–205.
[22] M. Bartholmai, R. Schriever, B. Schartel, Influence of external heat flux and coating thickness on thermal insulation properties of two different intumescent coatings using cone calorimeter and numerical analysis, Fire Mater. 27 (2003) 151–162.
[23] M.H. Khaneghahi, E.P. Najafabadi, P. Shoaei, A.V. Oskouei, Effect of intumescent paint coating on mechanical properties of FRP bars at elevated temperature, Polym. Test. 71 (2018) 72–86, https://doi.org/10.1016/j.polymertesting.2018.08.020.
[24] U. Sorathia, T. Gracik, J. Ness, A. Durkin, F. Williams, M. Hunstadt, F. Berry, Evaluation of intumescent coatings for shipboard fire protection, J. Fire Sci. 21 (2003) 423–450.
[25] T. Nosaka, R. Lankone, P. Westerhoff, P. Herckes, Flame retardant performance of carbonaceous nanomaterials on polyester fabric, Polym. Test. 86 (2020), 106497, https://doi.org/10.1016/j.polymertesting.2020.106497.
[26] A.R. Horrocks, A. Sitpalan, B.K. Kandola, Design and characterisation of bicomponent polyamide 6 fibres with specific locations of each flame retardant component for enhanced flame retardancy, Polym. Test. 79 (2019), 106041, https://doi.org/10.1016/j.polymertesting.2019.106041.
[27] A. Walther, I. Bjurhager, J.M. Malho, J. Ruokolainen, L. Berglund, O. Ikkala, Supramolecular control of stiffness and strength in lightweight high-performance nacre-mimetic paper with fire-shielding properties, Angew. Chem. Int. Ed. 49 (2010) 6448–6453.
[28] L. Berglund, A. Liu, Strong Nanopaper, 2010. Canada Patent Appl. PCT/SE2010/051259.
[29] A. Liu, A. Walther, O. Ikkala, L. Belova, L.A. Berglund, Clay nanopaper with tough cellulose nanofiber matrix for fire retardancy and gas barrier functions, Biomacromolecules 12 (2011) 633–641.
[30] F. Carosio, F. Cuttica, L. Medina, L.A. Berglund, Clay nanopaper as multifunctional brick and mortar fire protection coating - wood case study, Mater. Des. 93 (2016) 357–363.
[31] F. Carosio, J. Kochumalayil, A. Fina, L.A. Berglund, Extreme thermal shielding effects in nanopaper based on multilayers of aligned clay nanoplatelets in cellulose nanofiber matrix, Adv. Mater. Interfac. 3 (2016), 1600551.
[32] F. Carosio, J. Kochumalayil, F. Cuttica, G. Camino, L.A. Berglund, Oriented clay nanopaper from biobased components mechanisms for superior fire protection properties, ACS Appl. Mater. Interfaces 7 (2015) 5847–5856.
[33] A. Liu, L.A. Berglund, Fire-retardant and ductile clay nanopaper biocomposites based on montmorrilonite in matrix of cellulose nanofibers and carboxymethyl cellulose, Eur. Polym. J. 49 (2013) 940–949.
[34] S. Duquesne, S. Bourbigot, Flame retardant nonwovens, in: I.R. Chapman (Ed.), Application of Nonwovens in Technical Textiles, Woodhead Publishing Limited, New York, 2010.
[35] S. Nazaré, Fire protection in military fabrics, in: A.R. Horrocks, D. Price (Eds.), Advances in Fire Retardant Materials, Woodhead Publishing Limited, Cambridge, 2008, pp. 492–526.
[36] J.Y. Cheong, J. Ahn, M. Seo, Y.S. Nam, Flame-retardant, flexible vermiculite–polymer hybrid film, RSC Adv. 5 (2015) 61768–61774.
[37] J.A. Schaeffer, Mineral wool and vermiculite as insulation, Ind. Eng. Chem. 27 (1935) 1298–1303.
[38] S.A. Suvorov, V.V. Skurikhin, High-temperature heat-insulating materials based on vermiculite, Refract. Ind. Ceram. 43 (2002) 383–389.
[39] S. Takahashi, H.A. Goldberg, C.A. Feeney, D.P. Karim, M. Farrell, K. O'Leary, D. R. Paul, Gas barrier properties of butyl rubber/vermiculite nanocomposite coatings, Polymer 47 (2006) 3083–3093.
[40] A.B. Morgan, C.A. Wilkie, Flame Retardant Polymer Nanocomposites, John Wiley & Sons, Inc., Hoboken, New Jersey, 2007.
[41] W.E. Horn Jr., Inorganic hydroxides and hydrocarbonates: their function and use as flame-retardant additives, in: A.F. Grand, C.A. Wilkie (Eds.), Fire Retardancy of Polymeric Materials, Marcel Dekker, Inc., New York, 2000, pp. 285–352.
[42] T.R. Hull, A. Witkowski, L. Hollingbery, Fire retardant action of mineral fillers, Polym. Degrad. Stabil. 96 (2011) 1462–1469.
[43] P. Griss, H. Andersson, G. Stemme, Expandable microspheres for the handling of liquids, Lab Chip 2 (2002) 117–120.
[44] L. Jönsson, Expandable microspheres as foaming agent in thermoplastics, thermosets and elastomers, in: Blowing Agents and Foaming Processes, Munich, Germany, 2006.
[45] G. Camino, L. Costa, G. Martinasso, Intumescent fire-retardant systems, Polym. Degrad. Stabil. 23 (1989) 359–376.
[46] S. Bourbigot, M. Le Bras, S. Duquesne, M. Rochery, Recent advances for intumescent polymers, Macromol. Mater. Eng. 289 (2004) 499–511.
[47] G. Camino, R. Delobel, Intumescence, in: A.F. Grand, C.A. Wilkie (Eds.), Fire Retardancy of Polymeric Materials, Marcel Dekker, New York, 2000, pp. 217–243.
[48] G. Camino, S. Lomakin, Intumescent materials, in: A.R. Horrocks, D. Price (Eds.), Fire Retardant Materials, Woodhead Publishing, Cambridge, 2001, pp. 318–336.
[49] B. Schilling, Expandable graphite, Kunststoffe 87 (1997) 1004–1006.
[50] S. Duquesne, M. Le Bras, S. Bourbigot, R. Delobel, G. Camino, B. Eling, C. Lindsay, T. Roels, Thermal degradation of polyurethane and polyurethane/expandable graphite coatings, Polym. Degrad. Stabil. 74 (2001) 493–499.
[51] Nordmann Rassmann Gmbh, Expandable graphite used as fire barrier in plastics, Plastics, Addit. Compd. 2 (2000) 12.
[52] M. Modesti, A. Lorenzetti, F. Simioni, G. Camino, Expandable graphite as an intumescent flame retardant in polyisocyanurate–polyurethane foams, Polym. Degrad. Stabil. 77 (2002) 195–202.
[53] S. Ulah, F. Ahmed, A.M. Shariff, M.A. Bustam, The effect of 150 μm expandable graphite on char expansion of intumescent fire retardant coating, in: 3rd International Conference on Fundamental and Applied Sciences, ICFAS 2014, 2014, https://doi.org/10.1063/1.4898492.
[54] S. Duquesne, M. Le Bras, S. Bourbigot, R. Delobel, H. Vezin, G. Camino, B. Elling, C. Lindsay, T. Roels, Expandable graphite: a fire retardant additive for polyurethane coatings, Fire Mater. 27 (2003) 103–117.
[55] H. Sturm, B. Schartel, A. Weiss, B. Braun, SEM/EDX: Advanced investigation of structured fire residues and residue formation, Polym. Test. 31 (2012) 606–619, https://doi.org/10.1016/j.polymertesting.2012.03.005.
[56] C.V. Opelt, G.M. Candido, M.C. Rezende, Compressive failure of fiber reinforced polymer composites - a fractographic study of the compression failure modes, Mater. Today Commun. 15 (2018) 218–227.
[57] P. Luangtriratana, B.K. Kandola, S. Duquesne, S. Bourbigot, Quantification of thermal barrier efficiency of intumescent coatings on glass fibre-reinforced epoxy composites, Coatings 8 (2018) 347.
[58] P. Kosky, R. Balmer, W. Keat, G. Wise, Exploring Engineering, third ed., Academic Press, Waltham, 2013, pp. 259–281, chap 12 Mechanical Engineering.
[59] J.B. Henderson, J.A. Wiebelt, M.R. Tant, A model for the thermal response of polymer composite-materials with experimental-verification, J. Compos. Mater. 19 (1985) 579–595.
[60] J. Jin, Q.X. Dong, Z.J. Shu, W.J. Wang, K. He, Flame retardant properties of polyurethane/expandable graphite composites, 2014, Int. Confer. Perform. Based Fire Fire Protect. Eng. 71 (2013) 304–309, https://doi.org/10.1016/j.proeng.2014.04.044. Icpffpe 2013.